Heliyon 10 (2024) e27356

Contents lists available at ScienceDirect

Heliyon

journal homepage: www.cell.com/heliyon

Research article

Elucidation of clinical implications Arising from circadian rhythm and insights into the tumor immune landscape in breast cancer

Chunjie Sun [a,1], Hanyun Zhang [b,1], Ye Li [c], Yang Yu [c], Jingyang Liu [c], Ruijuan Liu [d,**], Changgang Sun [d,e,*]

[a] College of Traditional Chinese Medicine, Shandong University of Traditional Chinese Medicine, Jinan, 250355 Shandong, China
[b] College of First Clinical Medicine, Shandong University of Traditional Chinese Medicine, Jinan, 250355 Shandong, China
[c] Faculty of Chinese Medicine and State Key Laboratory of Quality Research in Chinese Medicines, Macau University of Science and Technology, Macau, Taipa, 999078, China
[d] Department of Oncology, Weifang Traditional Chinese Hospital, Weifang, 261041 Shandong, China
[e] College of Traditional Chinese Medicine, Shandong Second Medical University, Weifang, 261053 Shandong, China

ARTICLE INFO

Keywords:
Circadian rhythm
Circadian-related genes
Breast cancer
Tumor immune microenvironment
Immunotherapy

ABSTRACT

Background: Circadian rhythm is an internal timing system generated by circadian-related genes (CRGs). Disruption in this rhythm has been associated with a heightened risk of breast cancer (BC) and regulation of the immune microenvironment of tumors. This study aimed to investigate the clinical significance of CRGs in BC and the immune microenvironment.

Methods: CRGs were identified using the GeneCards and MSigDB databases. Through unsupervised clustering, we identified two circadian-related subtypes in patients with BC. We constructed a prognostic model and nomogram for circadian-related risk scores using LASSO and Cox regression analyses. Using multi-omics analysis, the mutation profile and immunological microenvironment of tumors were investigated, and the immunotherapy response in different groups of patients was predicted based on their risk strata.

Results: The two circadian-related subtypes of BC that were identified differed significantly in their prognoses, clinical characteristics, and tumor immune microenvironments. Subsequently, we constructed a circadian-related risk score (CRRS) model containing eight signatures (SIAH2, EZR, GSN, TAGLN2, PRDX1, MCM4, EIF4EBP1, and CD248) and a nomogram. High-risk individuals had a greater burden of tumor mutations, richer immune cell infiltration, and higher expression of immune checkpoint genes, than low-risk individuals, indicating a “hot tumor" immune phenotype and a more favorable treatment outcome.

Conclusions: Two circadian-related subtypes of BC were identified and used to establish a CRRS prognostic model and nomogram. These will be valuable in providing guidance for forecasting prognosis and developing personalized treatment plans for BC.

* Corresponding author. Department of Oncology, Weifang Traditional Chinese Hospital, Weifang, 261041 Shandong, China. College of Traditional Chinese Medicine, Shandong Second Medical University, Weifang, 261053 Shandong, China.
** Corresponding author. Department of Oncology, Weifang Traditional Chinese Hospital, Weifang, 261041 Shandong, China.
E-mail addresses: liuruijuan626@163.com (R. Liu), scgdoctor@126.com (C. Sun).
[1] These authors contributed equally to this work.

https://doi.org/10.1016/j.heliyon.2024.e27356
Received 7 October 2023; Received in revised form 3 February 2024; Accepted 28 February 2024
Available online 6 March 2024

1. Introduction

Breast cancer (BC) is the most prevalent malignancy in women and the leading cause of cancer-related deaths. BC incidence is increasing annually worldwide. Several epidemiological investigations have linked circadian disruptions, such as jet lag, disrupted sleep, and shift work, increasing the risk of BC [1–4]. Notably, many studies have verified that the circadian-related genes (CRGs) are a factor effecting the initiation, development, and prognosis of BC, by regulating physiological processes such as cell cycle control, cell proliferation, apoptosis, and DNA damage repair [5–9].

Recent findings have shown that circadian disruption affects the remodeling of the tumor immune microenvironment (TIME) and induces the establishment of an immunosuppressive microenvironment [10–12]. Historically, BC has been considered an immunologically "cold" tumor [13,14]. However, high throughput genomic and cellular profiling have indicated that the immunologic environment of BC is dynamic and heterogeneous, with a tumor microenvironment (TME) comprising unique functional immune infiltrates, suggesting potential new immunotherapeutic strategies [15–17]. Therefore, targeting analysis of the regulation of circadian rhythms on the BC immune microenvironment may provide an opportunity to diagnose and treat BC.

The circadian rhythm is a 24-h endogenous rhythm established by organisms to adapt to the Earth's rotation. As an important regulatory system for the maintenance of normal cell and tissue homeostasis, circadian rhythm plays a key role in processes associated with cancer [18–21]. This rhythm depends on the production of circadian genes and proteins regulated by the circadian clock. These genes can be specifically divided into core clock genes and clock control genes that interact with each other and affect the operation and expression of the circadian system [22–24]. Dysregulated or mutated circadian genes affect cancer development through complex and precise regulatory mechanisms, including regulation of the cell cycle, changes in metabolism, epithelial–mesenchymal transition, proliferation, and metastasis [5,25,26]. For example, the overexpression of *CLOCK* and *BMAL1* in BC tissues promotes the proliferation and invasion of BC cells [27–29]. Mutations in *NPAS2* are associated with BC risk [30,31].

Studies have shown that there is a strong association between CRGs and immune checkpoint inhibitors that can affect both the infiltration of immune cells into tumor patients and the TME [32]. Using a chronotherapy strategy to improve the benefit of immune checkpoint inhibitors may be sufficient to advance BC immunotherapy. In this strategy, CRGs could be a promising new set of biomarkers for BC risk and prognosis. Further research on CRGs is needed to realize precise and personalized medical regimens for BC.

In previous studies, Zhang et al. constructed a risk prediction model to classify BC patients into high- and low-risk groups through CRGs, which laid a certain foundation for our study [33]. We included more abundant CRGs and first identified the presence of different circadian subtypes in BC by consensus cluster analysis, which provided a reliable basis for model construction. A larger validation dataset was used, and after re-statistical analysis, our BC risk prediction model was constructed to distinguish between high-risk and low-risk groups of BC. The immune microenvironmental landscape of BC was mapped for a new perspective on circadian rhythms. In addition, the variance in gene mutations and biological processes between patients with different prognostic risks was further elucidated, which might provide new strategies for individualized healthcare.

2. Materials and methods

2.1. Data sources

The Cancer Genome Atlas (TCGA, https://tcga-data.nci.nih.gov/tcga/) and Molecular Taxonomy of Breast Cancer International Consortium (METABRIC, http://www.cbioportal.org) databases were used to describe the transcriptome and clinical characteristics of patients with BC. TCGA data were used for training purposes. METABRIC data were used as a validation set. To process the data, first, we removed the normal samples from the dataset. Then, we screened only those samples for which the survival time was >30 days, retaining only one sample per patient. Finally, we preserved genes that were detected in over fifty percent of the samples. CRGs were obtained from GeneCards [34] (http://www.genecards.org/) and MSigDB (http://software.broadinstitute.org/gsea/msigdb/index.jsp/). Local ethics committee approval was not required because the data were obtained from public databases (TCGA and METABRIC). The study strictly adhered to the data access policy and publication guidelines provided by TCGA and METABRIC [35,36].

2.2. Construction of circadian subtypes in BC

According to the expression of CRGs, the "ConsensusClusterPlus" was performed [37]. It could identify different circadian associated subtypes in BC. To assess the capacity of mRNA expression profiles in discriminating between the two types associated with the circadian rhythm, we conducted principal component analysis (PCA). The R packages "survival" and "survminer" were used to conduct survival analysis. For the identification of differentially expressed genes (DEGs) between the two isoforms, the R package "Limma" was used [38]. Technical support for the Sankey diagram was provided by the SangerBox platform (http://sangerbox.com/). Additionally, the association between different circadian-related clusters and clinical features, including age, survival status, and stage, was determined using the R package "pheatmap".

2.3. Enrichment analysis and immune landscape of circadian subtypes

In order to elucidate disparities in biological processes that exist in the two identified circadian subtypes, we performed gene set variation analysis (GSVA) using the "GSVA" R package [39]. Subsequently, DEGs were analyzed using Kyoto Encyclopedia of Genes and Genomes (KEGG), gene ontology (GO), and gene set enrichment analysis (GSEA) using "Clusterprofiler" [40–42]. We looked more

closely at how the infiltrating immune cells differed between the two subtypes with the help of "GSVA" and "GSEABase" R packages. The "ESTIMATE" calculated the immune, stromal, and estimated scores for the patients with BC [43]. To increase the precision of anticipating, the tumor immune dysfunction and exclusion (TIDE) tool (http://tide.dfci.harvard.edu/) was used to compare TIDE, microsatellite instability (MSI), dysfunction, and exclusion scores amongst various subtypes [44]. In addition, the "pRRophetic" R package screened commonly used drugs for BC to determine the potential sensitivity of chemotherapy and endocrine therapy drugs for different subtypes [45].

2.4. Construction and validation of circadian-related risk score (CRRS) model in BC

In breast cancer, core prognostic genes influence patient prognosis and immune function by regulating circadian rhythms. When the expression of these genes is dysregulated, circadian rhythm disruption may result. To investigate prognostic CRGs, univariate Cox regression analysis was performed utilizing the "survival". These prognostic CRGs were further analyzed. The "glmnet" was selected to perform a least absolute shrinkage and selection operator (LASSO) penalized Cox regression analysis [46]. Our goal is to identify genes that are important in predicting prognosis. The product of the expression of core prognosis-related CRGs and their coefficients yielded the CRRS. The formula for the risk score has been established as follows:

$$\mathrm{CRRS} = \sum_{i} \mathrm{Coefficient\ of\ (i)} \times \mathrm{Expression\ of\ gene\ (i)}.$$

The coefficient of the gene (i) is the regression coefficient of the gene (i), and the expression of the gene (i) is the expression value of gene (i) for each patient. Using the risk score formulation described above, patients in each cohort were classified into high- or low-risk groups using the median risk score as the cutoff value. The impact of multiple key CRGs on breast cancer prognosis was fully considered by CRRS, which was calculated to differentiate different risk groups, and to some extent visualized the status of circadian rhythm disruption in patients. High-risk patients had dysregulated expression of prognostic core genes, disrupted circadian rhythms, and worse prognosis compared to low-risk patients. Simultaneously, PCA and t-distributed stochastic neighbor embedding analyses were used to verify the reliability of the CRRS model in discriminating between different risk groups using the "Rtsne" R package. To check the reliability of the prediction model, the receiver operating characteristic (ROC) curve was plotted in the "survivalROC" R package. C-index was calculated by the R package "survcomp". Immunohistochemistry staining of prognostic CRGs was validated using the Human Protein Atlas (HPA; http://www.proteinatlas.org/) [47]. Risk scores, clinical events and model genes were presented using the SangerBox online platform (http://sangerbox.com/) [48].

2.5. Construction of the nomogram prediction model

Based on TCGA, the survival time, survival status, and other clinical characteristics of breast cancer patients were sorted out. Using the R packages "survival", "regplot" and "rms", a nomogram was created that is suitable for clinical use. After multifactorial Cox regression analysis, we can assess the extent to each independent variable (influencing factor) contributes to the outcome variables (e.g., survival time, survival status, etc.), i.e., the magnitude of the regression coefficients. The nomogram takes into account factors such as age, clinical stage and risk score. Points were assigned according to the level at which each independent variable was taken, and these scores were then summed to obtain a total points. To visualize these predictors, we integrated them and used scaled line segments, plotted on the same plane at a certain scale. Clinicians can use this intuitive linear scale to predict a patient's probability of survival at different time points, specifically 1-, 3-, and 5-year. Furthermore, the ROC curve and decision analysis (DCA) are also applied employing the "rmda" R package [49].

2.6. Mutation analysis

Mutational information were retrieved from TCGA and cBioPortal for Cancer Genomics (http://www.cbioportal.org) databases. To evaluate differences in the percentage of genomic modifications, mutation count, and TMB, the "Maftools" was used [50]. The median TMB was used to stratify the specimens. Then, for the purpose of survival analysis, we combined the risk score with the TMB score. In addition, the relationship between risk score and TMB was investigated. Information from the Gene Set Cancer Analysis (GSCA) website (http://bioinfo.life.hust.edu.cn/GSCA/) was used to identify mutations in core prognostic genes [51].

2.7. Functional enrichment analysis and evaluation of TIME

Initially, GO and KEGG analyses and GSEA were performed on DEGs between different risk groups. Based on potential gene signatures and the amount of each type of immune cell, the study examined the association between people at high risk and those at low risk using CIBERSORT. Using Spearman's correlation analysis, the association between signature genes and various immune cells was examined. The GSCA database was used to extract data on GSVA scores for these genes. This was then compared with immune functions, copy number variants (CNVs), and single nucleotide site variants (SNVs). Finally, variations in immune checkpoint gene expression and TIDE scores were compared between the high-risk and low-risk groups.

2.8. Statistical analyses

R software (version 4.0.5) was used to conduct statistical analysis. Groups were compared for differences in overall survival (OS) times using a bilateral log-rank test and a survival curve was constructed. To determine the P-values for the correlation study, Spearman's method was applied. More than two groups were compared using the Kruskal-Wallis test, whereas two groups were compared using the Wilcoxon test. We used the R q value function (included in the R package "q value") to compute Q-values in order to solve the problem of multiple hypothesis testing [52]. When $P < 0.05$, the results were deemed statistically significant.

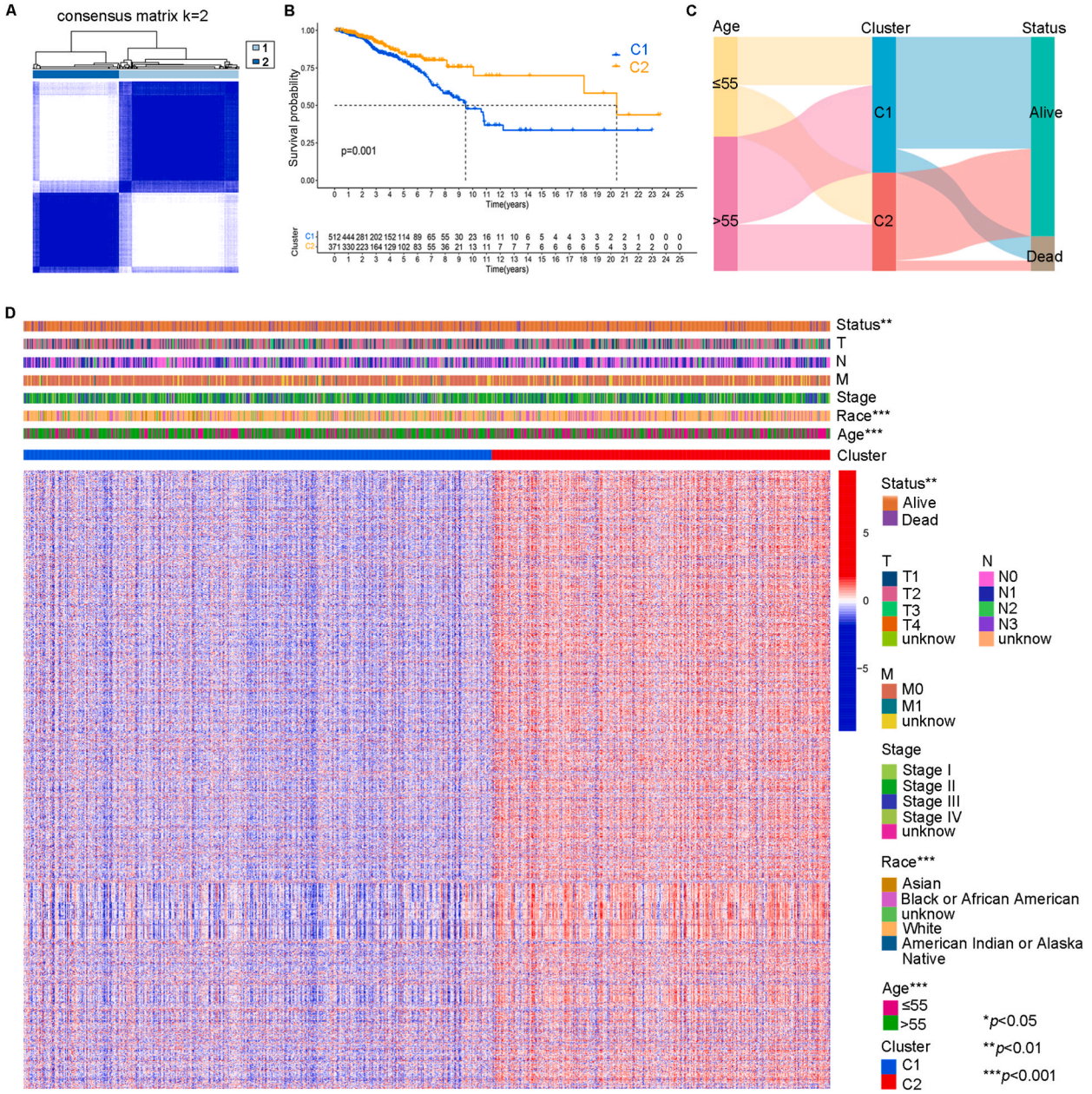

Fig. 1. Consensus clustering of circadian-related genes in BC in TCGA. (A) TCGA cohort patient consensus matrix. (B) KM curve for OS with circadian classes. (C) Alluvial diagram showing changes in age, circadian cluster, and survival status. (D) Unsupervised clustering of all circadian-related genes.

3. Results

3.1. Identification of circadian subtypes in BC

In the end, there were 1823 samples in the validation set and 883 samples in the training set. After gathering 2796 and 343 CRGs from GeneCards and MSigDB, respectively, duplicates were removed from the union of these sets. By intersecting the resulting set with the genes of patients with BC in TCGA, we identified 2655 CRGs. Unsupervised clustering with clusters 1 and 2 (512 and 371 cases, respectively) included in the training set was used to separate the two distinct circadian-related subpopulations based on CRG expression levels (Fig. 1A). PCA divided patients into two groups, confirming the presence of two diverse circadian-related subtypes (Supplemental Fig. 1A). To determine the variations in survival between clusters, BC cohorts in TCGA and METABRIC with relatively complete data on survival were examined. The survival advantage of Cluster 2 was greater than that of Cluster 1 (Fig. 1B,

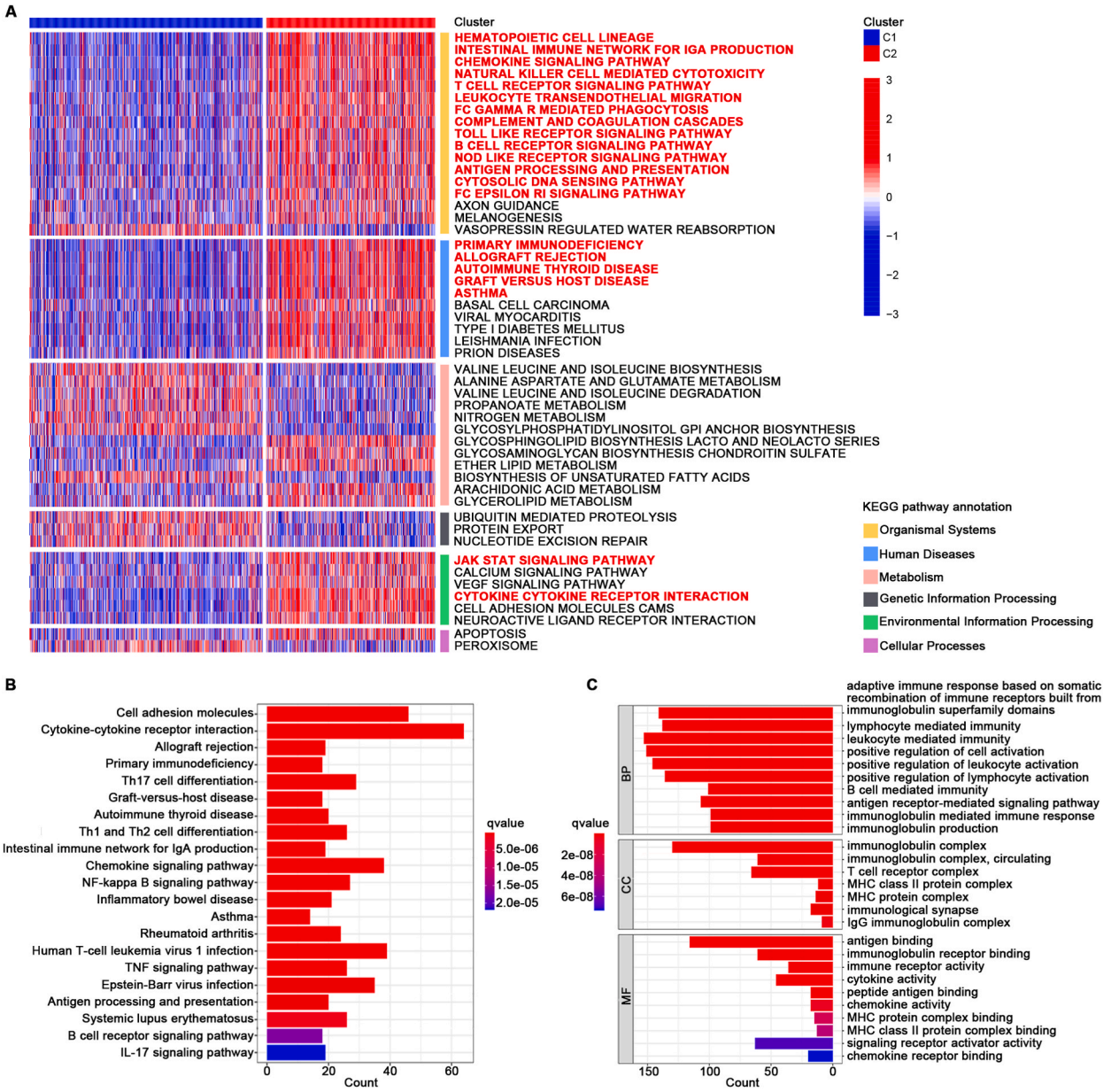

Fig. 2. Functional annotation analysis of DEGs between different circadian subtypes in TCGA. (A) GSVA data of the biological pathways. Immunologically relevant pathways: highlight in bold red font. Blue: inhibition of biological pathways. Red: activated biological pathways. (B) The analysis of KEGG enrichment in two circadian subtypes. (C) GO analysis of differentially expressed genes between two circadian subtypes. (For interpretation of the references to colour in this figure legend, the reader is referred to the Web version of this article.)

Supplementary Fig. 1B). Subsequently, associations between both groups and numerous clinical features were assessed (Fig. 1C). In contrast to Cluster 1, Cluster 2 had a larger percentage of patients aged ≤55 years and survival outcomes. Chi-square test findings revealed significant variations in many clinical aspects (Fig. 1D). These findings suggest that CRGs influence tumor development. Using a heat map, we identified two distinct circadian subtypes based on their transcriptomic profiles (Fig. 1D).

3.2. Immune landscape of circadian subtypes

GSVA was used to ascertain how the pathway enrichment analysis differed between the two circadian clusters in the TCGA cohort. According to the enrichment map, Cluster 1 was mainly focused on metabolic pathways and Cluster 2 was significantly enriched in

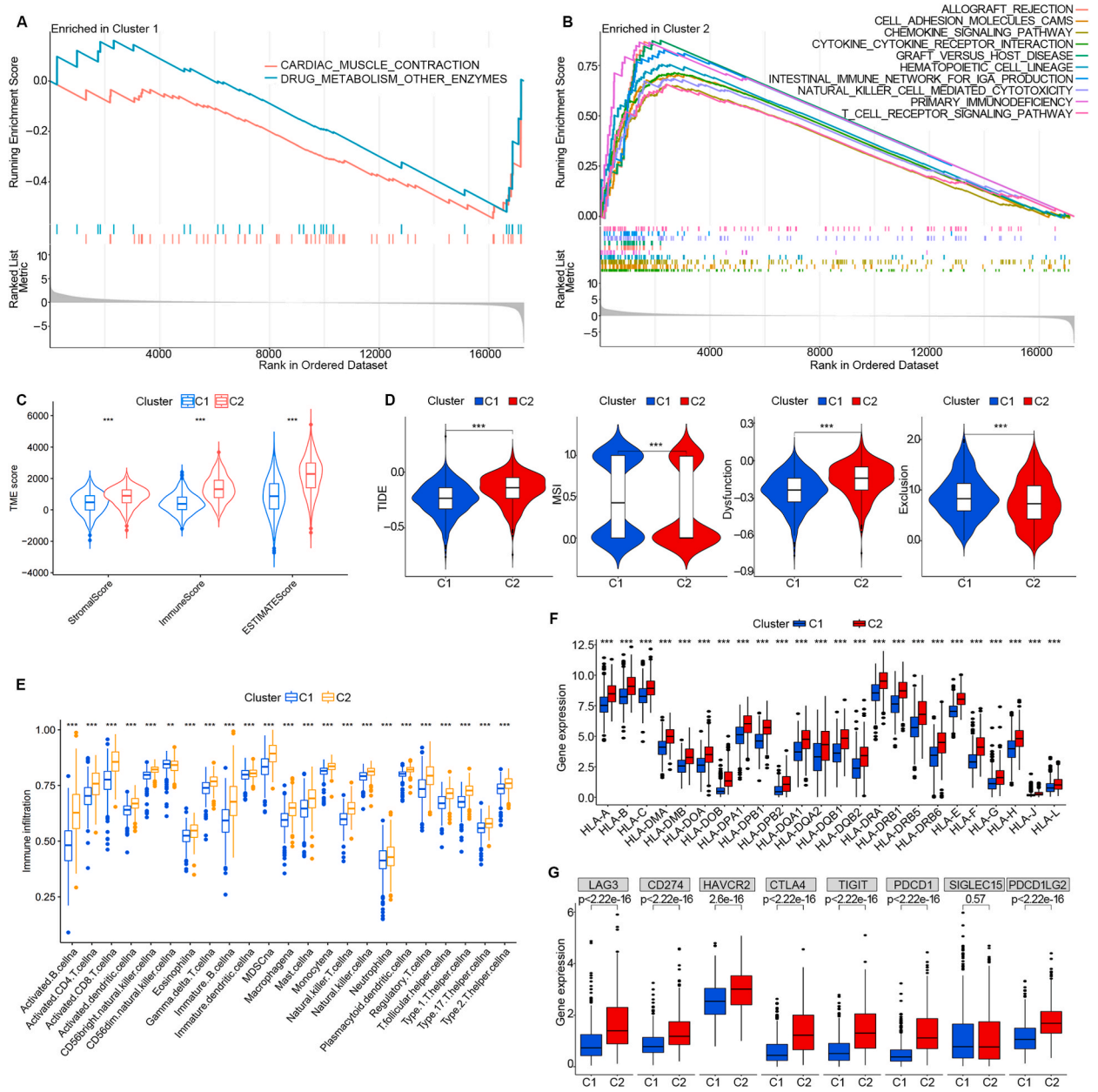

Fig. 3. Immune landscape and immunotherapy response prediction for circadian subtypes in the TCGA cohort. (A, B) GSEA of the functional pathways enriched in the two circadian subtypes. (C) Expression of stromal, immune, and estimate scores in the two circadian subtypes. (D) TIDE, MSI, dysfunction, and exclusion scores between both circadian subtypes. (E) The box plot shows the difference in immune cell infiltration between two circadian subtypes. (F) Differences in HLA-related gene expression levels. (G) Differential expression of immune checkpoint molecules in two circadian subtypes. Statistical significance expressed as ns ≥ 0.05, * <0.05, ** <0.01, *** <0.001, and **** <0.0001.

immune and inflammatory pathways (e.g., chemokine, T-cell receptor, B-cell receptor, and Toll-like receptor) (Fig. 2A). KEGG and GO analyses of the DEGs between the two circadian subtypes also revealed enrichment in immune function pathways (Fig. 2B and C). With this finding further confirmed by GSEA, Cluster 2 was significantly enriched in T-cell receptor, cell adhesion molecules, and chemokine signaling pathways (Fig. 3A and B). The ESTIMATE algorithm was used to further analyze the immune microenvironment of the two subtypes of BC by generating stromal, immune, and estimated scores. Cluster 2 had higher scores than Cluster 1 in all categories (Fig. 3C). Finally, we tested whether circadian subtypes were significantly correlated with the effects of immunotherapy. TIDE analysis revealed that Cluster 2 was associated with higher TIDE, MSI, and T-cell dysfunction scores than Cluster 1, while the opposite was

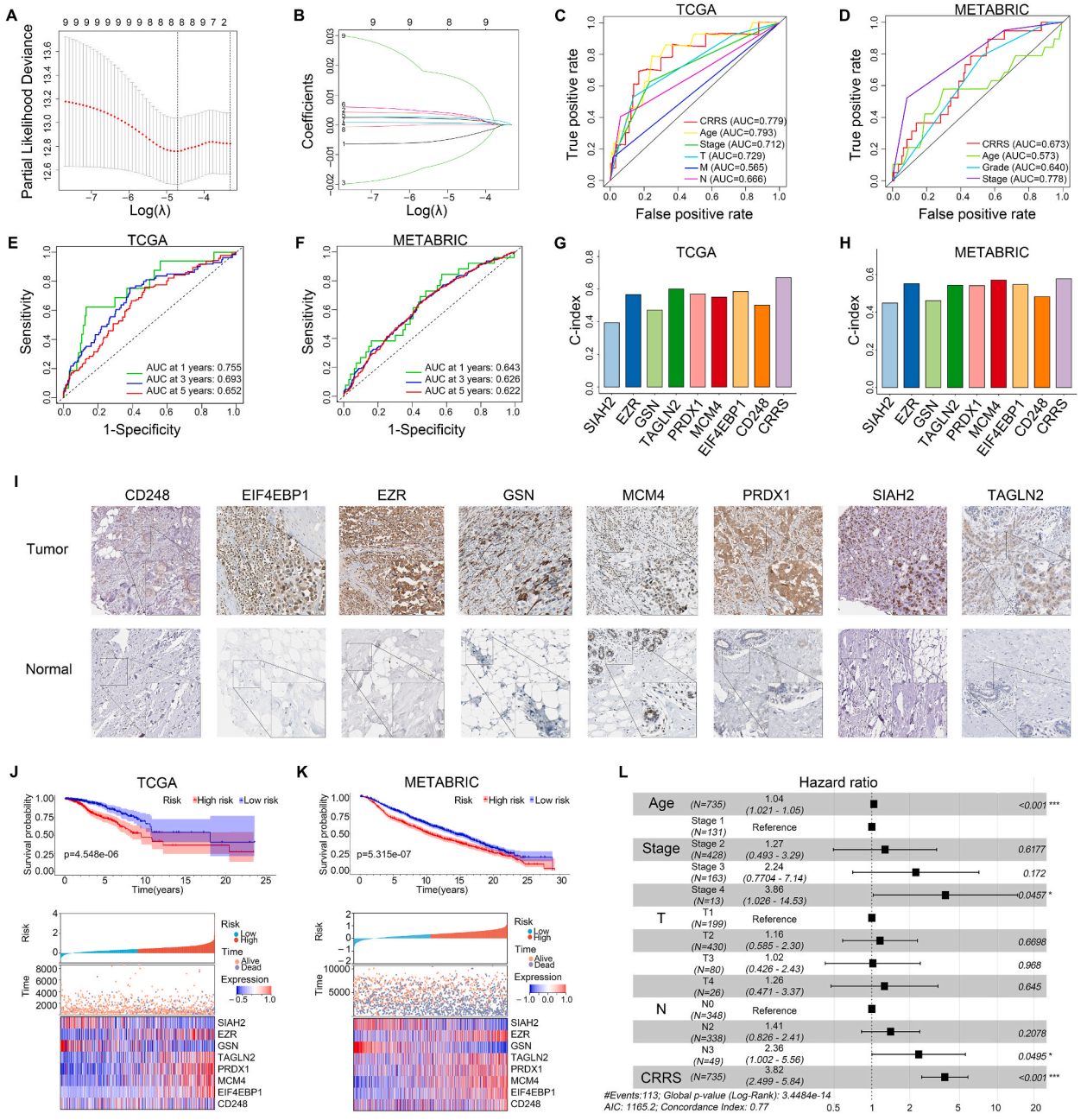

Fig. 4. Construction of CRRS model in BC. (A) LASSO-Cox regression to identify the best parameters. (B) LASSO coefficient profiles. (C, D) ROC curve analysis of the CRRS model, age, stage, and TNM stage in TCGA and METABRIC cohorts. (E, F) Time-dependent ROC curves of CRRS model prediction of 1-, 3-, and 5-year survival rates in TCGA and METABRIC. (G, H) C-indexes of regression models for CRRS and eight prognostic molecules in TCGA and METABRIC. (I) Differential gene expression of eight prognostic markers at the protein level. (J, K) KM curves of OS, risk scores, clinical events, and model genes between the two risk groups in TCGA and METABRIC. (L) Forest plot showing the prognostic impact of risk score and clinical factors.

observed for the T-cell exclusion scores (Fig. 3D). Due to the intriguing findings, we conducted further analysis on the correlation between different clusters and cancer-associated fibroblasts (CAFs). Additionally, Cluster 1 CAF signature genes with elevated expression levels were included in the investigation (Supplementary Fig. 2). Upon comparing the immune cell infiltration of both kinds, Cluster 2 had a unique immunological profile. Cluster 2 showed increased infiltration of natural killer cells and activated dendritic cells compared to Cluster 1 (Fig. 3E). Human leukocyte antigen (HLA) and immune checkpoint molecules play crucial roles in immune function and have significant clinical immunotherapy implications. Therefore, we also compared the expression levels of HLA and immune checkpoint genes among the different subtypes. Compared to Cluster 1, Cluster 2 has higher levels of HLA molecule expression (Fig. 3F). Comparative analysis of immune checkpoint gene expression suggested that Cluster 2 may have a more positive response to immunotherapy against the CTLA4, CD274, LAG3, TIGIT, HAVCR2, PDCD1, and PDCD1LG2 immune checkpoints (Fig. 3G). Furthermore, the prediction of sensitivity to chemotherapeutic drugs in different subtypes was performed in this study (Supplementary Fig. 3). Among them, cyclophosphamide, paclitaxel, vinorelbine, gemcitabine, cisplatin, 5-fluorouracil, epirubicin and docetaxel, which are commonly used in breast cancer chemotherapy, showed more benefit in Cluster 1 (Supplementary Fig. 3A).

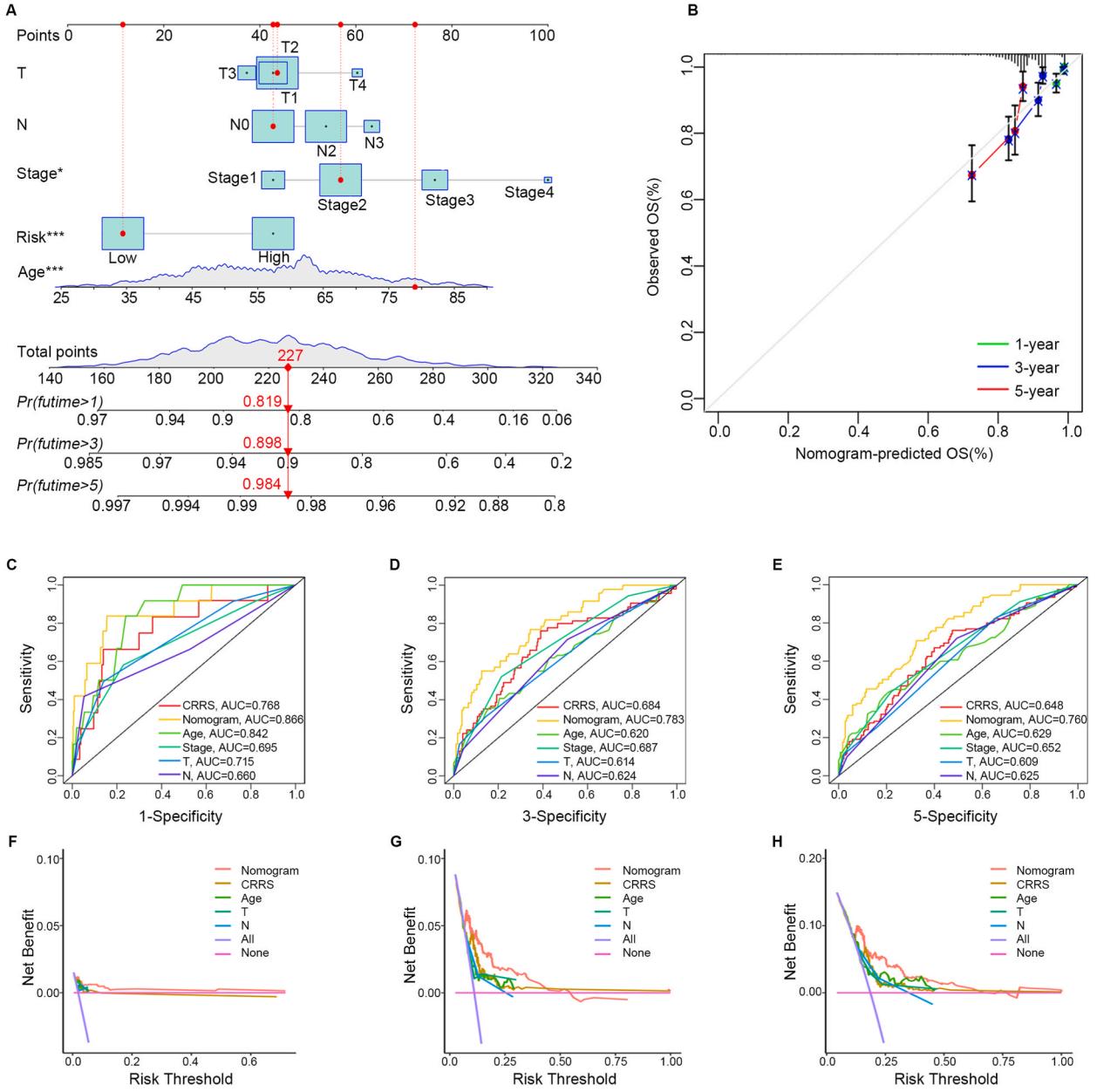

Fig. 5. Construction of nomograms based on CRRS model with clinical characteristics. (A) Predictive nomograms. (B) Calibration curves of the nomogram. (C–E) AUC of nomograms predicting 1, 3, and 5 year OS probabilities. (F–H) DCA graphs for 1, 3, and 5 year survival.

Cluster 1 also has advantages in endocrine therapy, such as tamoxifen and fulvestrant (Supplementary Fig. 3B). Overall, our findings suggest that Cluster 2 patients, with increased HLA molecule expression and a unique immunological profile, may respond better to immunotherapy targeting specific immune checkpoints. These findings further underline the importance of understanding the role of the TIME in circadian-related disorders and their potential implications for therapeutic strategies.

3.3. Circadian-related signatures for prognostic prediction of BC

To provide personalized medical decision-making support, we established a prognostic model based on CRGs. A stable eight-gene panel (*SIAH2*, *EZR*, *GSN*, *TAGLN2*, *PRDX1*, *MCM4*, *EIF4EBP1*, and *CD248*) was selected and output as CRRS signatures using LASSO Cox regression analysis for patients with BC with survival information in the training and validation cohorts (Fig. 4A and B). Finally, a formula for the CRRS model for the prognostic assessment of BC was obtained: $CRRS = (-0.0043 \times SIAH2) + (0.0030 \times EZR) + (-0.0109 \times GSN) + (0.0006 \times TAGLN2) + (0.0023 \times PRDX1) + (0.0036 \times MCM4) + (0.0019 \times EIF4EBP1) + (0.0155 \times CD248)$. ROC curve and C-index components of the Cox regression model were used to evaluate the predictive ability. Compared with that of other clinical models, the area under the ROC curve (AUC) of the CRRS model was 0.779 and 0.673 in TCGA and METABRIC cohorts, respectively, which demonstrated the good prognostic prediction efficiency of the combined model (Fig. 4C and D). Subsequently, time-dependent ROC analyses were performed on patients with BC from different cohorts at 1, 3, and 5 years of follow-up. The time-based AUC was >0.6 for both cohorts (Fig. 4E and F). Of note, the AUC of the 1-year ROC curve in TCGA was 0.755, which means that the prognostic risk score demonstrated good predictive power. In addition, the combined model had the highest C-index compared with other univariate Cox regression models (Fig. 4G and H). These results further clarify that a prognostic model with eight circadian rhythm-related features is required for accurate prognostic predictions.

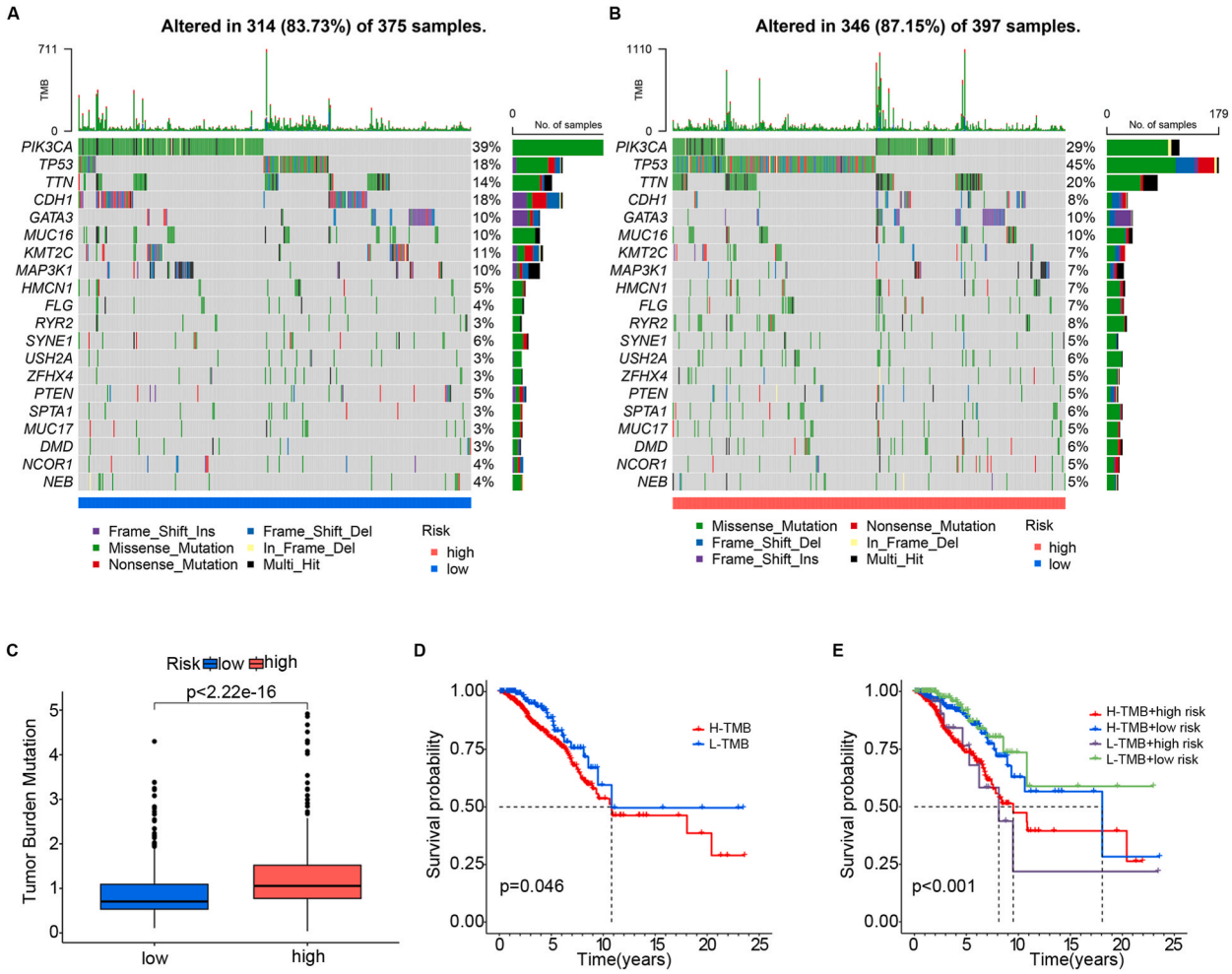

Fig. 6. Somatic mutations in different risk groups based on CRRS model. Somatic mutations in the low-risk (A) and high-risk (B) groups. (C) TMB analysis between the high- and low-risk groups. (D) KM curve compares the overall BC patients between the high- and low-mutation groups. (E) KM curve based on mutation and risk scores for the four subgroups compared with overall BC patients.

We searched the HPA database for the eight prognostic genes of the CRRS model. Consistent with our expected results, the expression of these genes was different at the protein level between BC and normal tissues. The findings may indicate new candidate biomarkers and therapeutics targeting opportunities in clinical diagnosing and treatment of BC (Fig. 4I). After calculating the CRRS, patients were categorized as either high or low risk according to the median score. In both TCGA (log-rank test P = 4.548*e−6) and METABRIC (log-rank test P = 5.315*e−7) cohorts, survival analysis showed that the low-risk population had a superior outcome (Fig. 4J and K). Risk scores, survival status and the expression levels of the eight risk genes are also displayed. A higher number of mortality cases was observed in the high-risk group, and there were significant differences in the expression levels of the eight

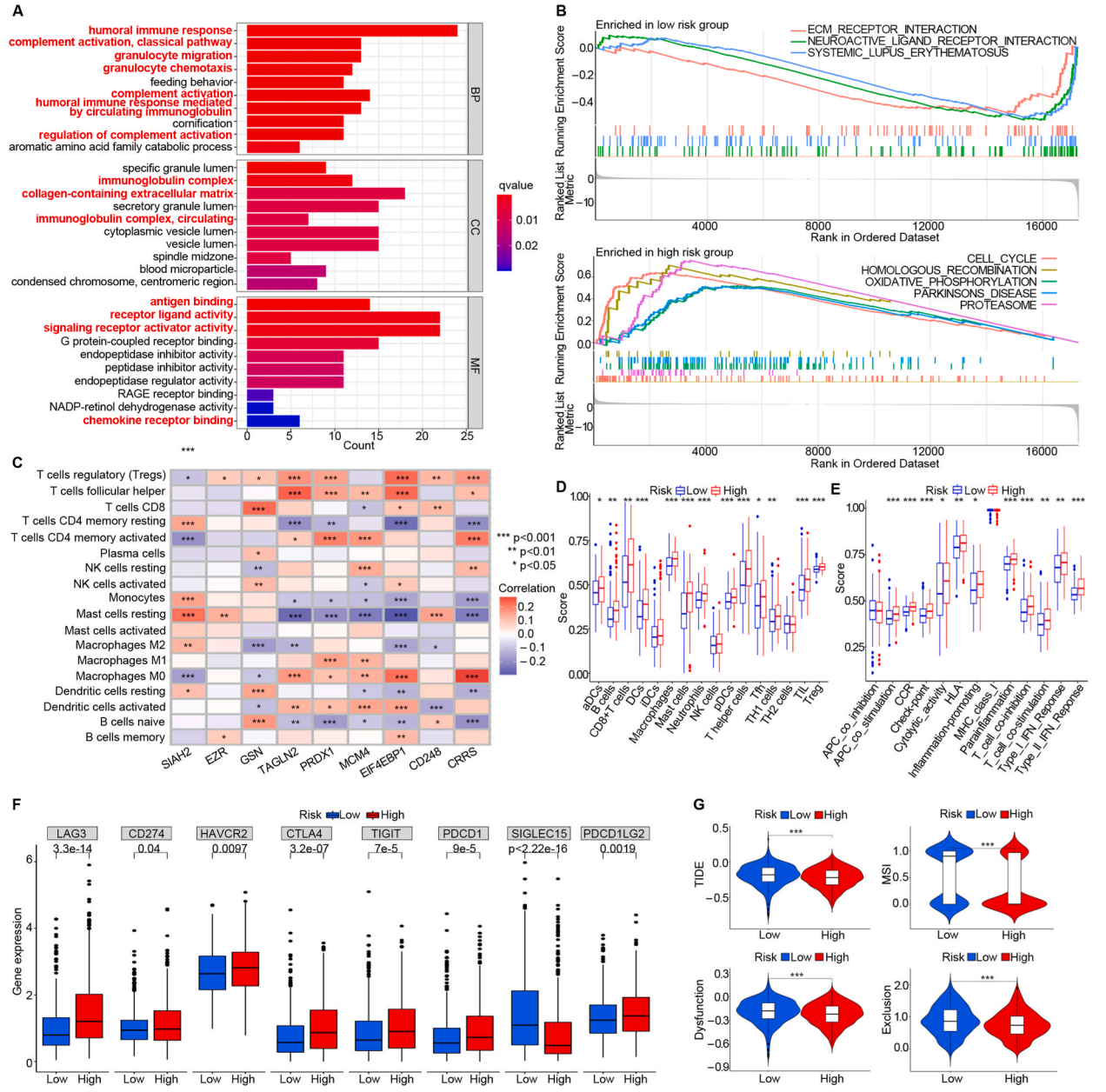

Fig. 7. Evaluation of the immune landscape and treatment response. (A) GO enrichment analysis. Immune related biological process, cell component and molecular function are highlighted in bold in red. (B) GSEA enrichment plots based on KEGG gene sets. (C) Association between CRRS signature expression and immune cell infiltration level. Comparison of differences in immune cell infiltration (D), immune cell and immune function ssGSEA scores (E) between high- and low-risk groups. (F) Immune checkpoint molecule expression is different among different populations. (G) The comparisons of the TIDE, MSI, dysfunction, and exclusion scores. Statistical significance expressed as ns ≥ 0.05, * <0.05, ** <0.01, *** <0.001, and **** <0.0001. (For interpretation of the references to colour in this figure legend, the reader is referred to the Web version of this article.)

prognostic genes between the high-risk and low-risk group (Fig. 4J and K). Multivariate Cox analysis showed that in addition to CRRS, age, stage 4, and N3 were also prognostic factors, which may help develop personalized treatment plans or make a more accurate prognosis evaluation (Fig. 4L).

3.4. Nomogram construction and evaluation

To give a method for statistically predicting the 1-, 3-, and 5-year OS probability of BC, a nomogram on the basis of risk score, stage, age, and other parameters was created (Fig. 5A). The calibration study showed that the nomogram plot exhibited exceptional stability and patient OS prediction curves at 1-, 3-, and 5-year closely resembled the optimal 45-degree calibration lines (Fig. 5B). Subsequently, time-dependent ROC analyses were performed to compare AUC values for the nomogram, risk score, and other clinical parameters. At 1-, 3-, and 5-year, all nomograms' time-dependent ROC curves had an AUC greater than 0.75, with a particularly high 1-year AUC of 0.866 (Fig. 5C–E). DCA was also used to test the prediction model and the nomogram was better at predicting OS than the other models (Fig. 5F–H). On the basis of this clinical feature, the combination of our risk models is a more valuable guide for the prediction of the prognosis of women with BC.

3.5. Multi-omics mutation analysis based on CRRS model

Multi-omics mutation analysis based on the CRRS model can identify specific genomic changes related to the circadian rhythm of BC, and could lead to more precise and individualized therapeutic strategies for patients with BC. Previous research has shown that somatic mutations are associated with poor outcomes in BC [53–56]. We investigated the differences in the distribution of somatic mutations between populations at different risk levels. The occurrence rate of somatic mutations was comparatively reduced in the low-risk cohort (83.73%) as opposed to that in the high-risk cohort (87.15%), as was evident from the visualization of the top 20 genes with the highest mutation frequencies in both patient groups (Fig. 6A and B). *PIK3CA*, *TP53*, and *TTN* exhibited the utmost mutations were the most frequent. Moreover, substantial dissimilarity in TMB was observed in both risk groups (Fig. 6C). The analysis unveiled a notable disparity in prognosis between the high- and low-TMB groups (Fig. 6D). Combining the risk score with TMB, a striking observation emerged; patients belonging to the low-TMB and low-risk subgroups exhibited a considerably more favorable prognosis than those in the other subgroups (Fig. 6E). Additionally, the prevalence of CNV within the risk signature was investigated, with the exception of EZR, which was a deletion; the remaining seven genes were amplified (Supplementary Fig. 4A). The percentage of CNV and the chromosomal locations and mutation patterns of genes within the CRRS model are shown (Supplementary Fig. 4B and C). To elucidate the biological mechanisms that contribute to the abnormal expression of CRRS model genes in patients with BC, we investigated SNVs within the risk signatures present in tissue samples [57]. Analysis of the findings revealed that patients with BC were most prone to missense mutations, with single nucleotide polymorphisms being the prevalent form of variation (Supplementary Fig. 4D). Notably, SNV predominantly involved C > T and C > G alterations (Supplementary Fig. 4D). A risk signature for somatic mutations was present in 21 patients with BC, with the highest frequencies in *MCM4* and *CD248* (Supplementary Fig. 5A). In addition, determination of the Spearman's correlation coefficient for CNV and gene expression analysis revealed increases in CNV for *MCM4*, *EZR*, *TAGLN2*, *EIF4EBP1*, *PRDX1*, and *GSN* (Supplementary Fig. 5B). We further explored the homozygous and heterozygous mutation profiles of prognostic genes. Homozygous copy number amplification occurred mainly in *EIF4EBP1* and *TAGLN2*, whereas *EZR* mainly manifested as a deletion. Heterozygous mutations were mainly *TAGLN2* and *MCM4* amplifications, whereas *EZR*, *PRDX1*, and *GSN* showed copy number reduction. The findings indicate that aberrant gene expression may be secondary to CNV and SNV (Supplementary Fig. 5C).

3.6. Multi-omics immunoassay based on CRRS model

Disruptions in circadian rhythms promote tumor growth by affecting the regulation of immune responses [11]. To elucidate the biological functions and pathways linked to CRRS, a series of pathway enrichment analyses were performed. GO analysis demonstrated a notable enrichment of DEGs in the biological processes relevant to immunity, such as complement activation, humoral immune response and granulocyte migration. Additionally, the DEGs were significantly correlated with immunity in terms of cellular components and molecular functions (Fig. 7A). KEGG enrichment analysis highlighted a robust correlation between DEGs and signaling pathways related to interleukin-17, cell cycle regulation, and metabolic processes (Supplementary Fig. 6A). Based on this, GSEA was used to gain a better understanding of the variations in enrichment pathways. Our findings revealed that the low-risk group exhibited enrichment in extracellular matrix receptor interactions, neuroactive ligand receptor interactions, and systemic lupus erythematosus. The high-risk group demonstrated enrichment in cell cycle, homologous recombination, oxidative phosphorylation, Parkinson's disease, and proteasomes (Fig. 7B). Taken together, these results reveal a correlation between the CRRS model and tumor immunity.

Immunotherapy is increasingly used in BC. The study of the TME will help to discover new targets and mechanisms for the immunotherapy of BC [58]. We found that the risk score and eight genes in the CRRS model were strongly correlated with immune cells (Fig. 7C). With respect to the gene set, mRNA expression and dendritic cells, B cells, macrophages, NK cells, and T helper type 1 were positively linked to the infiltration scoring. Negative correlations were observed with T helper type 17, neutrophils, naturally occurring T regulatory cells, CD4 naïve T cells, and CD4 T cells (Supplementary Fig. 6B). In addition, the CNV gene set showed a higher infiltration of CD4 naive T cells, B cells, and CD8 T cells, among others, compared to the wild-type gene set (Supplementary Fig. 6C). The SNV gene set exhibited a higher infiltration of effector memory T cells compared to the wild type (Supplementary Fig. 6C). The disruption of circadian rhythms can also lead to abnormalities in the number and proportion of certain types of immune cells, creating

an environment conducive to tumor proliferation. The high-risk group had a markedly higher concentration of mast cells, dendritic cells, $CD8^+$ T cells, macrophages, plasma-like dendritic cells, and many other cells compared to the low-risk group (Fig. 7D). The high-risk group displayed elevated immune function scores, including checkpoint, cytolytic activity, HLA, inflammatory promotion (Fig. 7E).

BC treatment has been transformed by the introduction of immune checkpoint inhibiting therapy [59]. The findings revealed a substantial increase in the levels of immune checkpoint genes expressed in the high-risk cohort, including widely recognized genes such as *CTLA4*, *CD274*, *LAG3*, and *TIGIT* (Fig. 7F). For both the high- and low-risk populations, the TIDE score, MSI score, T-cell exclusion and T-cell dysfunction were also calculated. For each parameter, the low-risk group exhibited higher values than the high-risk group, underscoring the possibility of greater resistance to immunotherapy and a propensity for immune evasion in the former group (Fig. 7G). Therefore, it can be concluded that high-risk cohorts possess greater potential for immunotherapy.

4. Discussion

BC is a highly heterogeneous disease, with multiple genetic, environmental, and lifestyle factors involved in its pathogenesis, the precise mechanisms of which have not been completely defined [60]. Increasing evidence suggests that circadian rhythms regulate physiological processes like cell cycle, metabolism, and immune function, thereby influencing BC risk, progression, and prognosis [61–64]. Therefore, we investigated the risk, prognosis, and immunological microenvironment of BC from the perspective of CRGs.

With regard to the acquisition of CRGs, we wanted to be as complete and accurate as possible. Therefore, we collected 2655 CRGs from the MSigDB and GeneCards databases. Using bioinformatic methods, we identified two subtypes of circadian association in BC and found that the prognosis, clinical characteristics, and immune microenvironment of these two subtypes were significantly different. According to the analysis of clinical characteristics, patients in Cluster 1 had poorer prognostic outcomes than those in Cluster 2, and Cluster 1 had a higher proportion of patients aged >55 years. The intrinsic molecular mechanisms underlying this discrepancy were investigated using GSVA, GO and KEGG analyses, and GSEA. Clusters 1 and 2 were significantly enriched in metabolic, inflammatory, and immune pathways, with particular differences in immune function. Cluster 2 showed a definite advantage in immune cell infiltration when we looked more closely at the variations in tumor immune cell infiltration of the two kinds. Compared to Cluster 1, Cluster 2 had a much better immunological score and a greater immune cell count. As is widely known, on the basis of the microenvironments of tumors, two main types have been previously distinguished: hot tumors, which have a high immune infiltration, and cold tumors, which have a low immune cell infiltration [65,66]. Hot tumors benefit from immunotherapy [67]. In the present study, the analysis was continued and differences in HLA and immune checkpoint gene expression levels between the two subtypes were identified. The results confirmed that Cluster 2 may be a hot tumor and Cluster 1 a cold tumor. To further verify our hypothesis, we compared the TIDE scores. Interestingly, TIDE, MSI, and T-cell dysfunction scores were higher in Cluster 2 than in Cluster 1, whereas the opposite was true for the T-cell exclusion score. This suggests that Cluster 2, although a hot tumor, their immunotherapeutic efficacy may be compromised by T-cell dysfunction and tumor immune escape. Cluster 1 demonstrated a close association between cold tumors and the enrichment of cancer-associated fibroblasts. Accumulation of these fibroblasts in the BC microenvironment forms a dense extracellular matrix, establishes chemical and physical barriers to promote T-cell rejection, and induces an immunosuppressive microenvironment, promoting the transformation and progression of the TME into a cold tumor [68–71].

Two distinct circadian subtypes of BC exist, suggesting that patients might have different prognoses. We successfully constructed an eight-signature BC CRRS prognostic model to accurately identify patient groups with different risk stratification. This model has been extensively validated and has been shown to be one of the most independent and important factors in the assessment of the prognosis of BC. This can be used to better understand patient outcomes and target medical interventions more accurately. In addition, we developed a nomogram combining the CRRS prognostic model and clinicopathological features as an easy-to-use and individualized clinical tool to help doctors make informed treatment decisions. The linear scale and nomogram are user-friendly tools that simplify the calculation process. They can help physicians comprehend and become proficient with the model, making it easier to diagnose a patient's illness and increasing the effectiveness of diagnosis and therapy. Additionally, nomogram results can be shared among multidisciplinary teams, enhancing patient care efficiency and ultimately reducing time and costs. Clear and objective visual aids help patients and their families understand their condition and prognosis, and ease communication with their doctor. They improve the doctor-patient relationship, patient satisfaction, and engagement. ROC, calibration, and decision curves were used to verify the performance of the nomogram. Based on previous reports, the CRRS model indicates a strong association between all eight signatures and the incidence and development of BC. Specifically, genes like *CD248*, *MCM4*, *EIF4EBP1*, *SIAH2*, *EZR* and *GSN* promote BC cell migration and invasion [72–79]. When these genes are highly expressed, they tend to be associated with a worse BC prognosis. Conversely, downregulation of *TAGLN2* expression in BC is associated with a poorer prognosis [80,81]. Of particular interest is *PRDX1*, it can act as a tumor suppressor in breast malignancies while simultaneously protecting malignant cells from immediate death and promoting cancer growth [82–84]. The protein levels of these prognostic genes in cancerous and normal breast tissues was confirmed by immunohistochemistry using the HPA database.

As cancer treatment enters the era of precision medicine, molecular targeted therapy and immunotherapy are emerging and BC treatment has improved by leaps and bounds. We sought breakthroughs in mutation and immune microenvironment through multi-omics analysis to understand the forecasting ability of the CRRS prognostic model in individuals diagnosed with BC, determine the underlying molecular mechanisms, and explore personalized precision interventions.

Somatic mutations are critical to breast cancer development and progression. Mutation analysis is widely used in clinical practice because of its broader range of uses compared to other histological analyses, and most clinical guidelines are based on single-gene

mutations. Consistent with previous findings, BC patients with a higher somatic mutation frequency and TMB had a worse prognosis. We also found that the high-risk group had a higher TMB and may benefit from immune checkpoint blockade therapy, as TMB has been shown to be a biomarker for patients who benefit from immunotherapy [85,86]. After CNV, SNV, mutation type, and genotype analyses, we found that prognostic genes were more likely to have missense mutations. Single nucleotide polymorphisms are a common type of variation. *MCM4* and *CD248* were the most frequently mutated of the eight genes. Homozygous mutations refer to the presence of the same mutation in both alleles of the same gene, whereas heterozygous mutations refer to the presence of different mutations in each allele. Analysis of these different types of mutations can help determine the genetic status of patients carrying disease-causing mutations.

GO, KEGG, GSEA, and GSCA data revealed a strong correlation between the CRRS model and tumor immunity. Immune cell infiltration and function analyses showed that the high-risk group performed significantly better than the low-risk group. As expected, the high-risk group had a good therapeutic response to multiple immune checkpoint inhibitors. This was confirmed by the TIDE score. Despite the terrible prognoses of the patients in the high-risk category, our findings showed that they had a hot tumor immune phenotype, which is a brighter picture for their treatment. In conclusion, identifying high and low-risk patient groups using a risk model and promptly applying appropriate treatment strategies will improve patient's prognoses and quality of life. For high-risk patients, immunotherapy strategies, particularly immune checkpoint inhibitors, offer better treatment outcomes and prognosis. Furthermore, patients at high risk necessitate more frequent monitoring and follow-up, as well as closer medical management to promptly respond to any potential disease progression or recurrence.

Although the CRRS prognostic model and nomogram that we constructed can provide a more accurate prognosis and personalized treatment for patients with BC, there are some limitations of this study. To begin with, our research relies on the examination of data from open sources, which could cause forecasts to differ from the real world. For example, in an era when immunotherapy and molecularly targeted therapies have not yet been fully developed, public databases collect limited information on the treatments received by patients, which may have an impact on survival. And second, although the response to immunotherapy has been predicted by immune checkpoint genes and TIDE scores, more treatment data from larger BC-related immunotherapy cohorts is needed for an in-depth understanding and expansion of the field.

To sum up, our work discovered two circadian subtypes of BC and constructed a CRRS prognostic model and nomogram to predict BC prognosis, which promoted the understanding of the clinical significance of circadian rhythm in breast cancer and guided individualized treatment for different patients. Additionally, we have studied the relationship between different populations and somatic mutations and time differences. These findings provide a new perspective on understanding the genetic basis of breast cancer patients and predicting their response to immunotherapy.

Ethics statement

As the data were obtained from public databases (TCGA and METABRIC), local ethics committee approval was not required. The study strictly adhered to the data access policy and publication guidelines provided by TCGA and METABRIC.

Funding statement

This study was supported by the National Natural Science Foundation of China (No. 82174222, 81973677), Natural Science Foundation of Shandong Province (ZR2021LZY015), Traditional Chinese Medicine Science and Technology Project of Shandong Province (Z-2022021) and Qingdao Municipal Science and Technology Benefit the People Demonstration Project (23-2-8-smjk-1-nsh).

Data availability statement

All data in this study are available in TCGA, METABRIC, GeneCards, MSigDB, and HPA datasets.

CRediT authorship contribution statement

Chunjie Sun: Writing – review & editing, Writing – original draft, Visualization, Validation, Software, Data curation, Conceptualization. **Hanyun Zhang:** Writing – review & editing, Writing – original draft, Conceptualization. **Ye Li:** Writing – review & editing, Software, Methodology, Data curation. **Yang Yu:** Writing – review & editing, Methodology, Data curation. **Jingyang Liu:** Writing – review & editing, Data curation, Conceptualization. **Ruijuan Liu:** Writing – review & editing, Data curation, Conceptualization. **Changgang Sun:** Writing – review & editing, Resources, Conceptualization.

Declaration of competing interest

The authors declare that they have no known competing financial interests or personal relationships that could have appeared to influence the work reported in this paper.

Acknowledgments

Not applicable.

Abbreviations

BC	breast cancer
CRGs	circadian-related genes
TIME	tumor immune microenvironment
TME	tumor microenvironment
MSI	microsatellite instability
TIDE	tumor immune dysfunction and exclusion
PCA	principal component analysis
ROC	receiver operating characteristic
AUC	area under the curve
KEGG	Kyoto Encyclopedia of Genes and Genomes
GO	gene ontology
HPA	Human Protein Atlas
GSCA	Gene Set Cancer Analysis
GSEA	gene set enrichment analysis
GSVA	gene set variation analysis
HLA	human leukocyte antigen
CAFs	cancer-associated fibroblasts
DCA	decision curve analysis
TMB	tumor mutation burden
CRRS	circadian-related risk score
CNV	copy number variation
SNV	single nucleotide site variant
LASSO	least absolute shrinkage and selection operator
DEGs	differentially expressed genes
OS	overall survival
KM	Kaplan-Meier

Appendix A. Supplementary data

Supplementary data to this article can be found online at https://doi.org/10.1016/j.heliyon.2024.e27356.

References

[1] C. Schwarz, A.M. Pedraza-Flechas, R. Pastor-Barriuso, V. Lope, N.F. de Larrea, J.J. Jimenez-Moleon, M. Pollan, B. Perez-Gomez, Long-term nightshift work and breast cancer risk: an updated systematic review and meta-analysis with special attention to menopausal status and to recent nightshift work, Cancers 13 (23) (2021).
[2] M. Szkiela, E. Kusidel, T. Makowiec-Dabrowska, D. Kaleta, Night shift work-A risk factor for breast cancer, Int. J. Environ. Res. Publ. Health 17 (2) (2020).
[3] E. Cordina-Duverger, F. Menegaux, A. Popa, S. Rabstein, V. Harth, B. Pesch, T. Bruning, L. Fritschi, D.C. Glass, J.S. Heyworth, T.C. Erren, G. Castano-Vinyals, K. Papantoniou, et al., Night shift work and breast cancer: a pooled analysis of population-based case-control studies with complete work history, Eur. J. Epidemiol. 33 (4) (2018) 369–379.
[4] S. Song, L. Lei, R. Zhang, H. Liu, J. Du, N. Li, W. Chen, J. Peng, J. Ren, Circadian disruption and breast cancer risk: evidence from a case-control study in China, Cancers 15 (2) (2023).
[5] M. Lesicka, E. Jablonska, E. Wieczorek, B. Peplonska, J. Gromadzinska, B. Seroczynska, L. Kalinowski, J. Skokowski, E. Reszka, Circadian gene polymorphisms associated with breast cancer susceptibility, Int. J. Mol. Sci. 20 (22) (2019).
[6] X. Lou, H. Wang, Y. Tu, W. Tan, C. Jiang, J. Sun, Z. Bao, Alterations of sleep quality and circadian rhythm genes expression in elderly thyroid nodule patients and risks associated with thyroid malignancy, Sci. Rep. 11 (1) (2021) 13682.
[7] E. Reszka, M. Przybek, O. Muurlink, B. Peplonska, Circadian gene variants and breast cancer, Cancer Lett. 390 (2017) 137–145.
[8] F. Okazaki, N. Matsunaga, H. Okazaki, H. Azuma, K. Hamamura, A. Tsuruta, Y. Tsurudome, T. Ogino, Y. Hara, T. Suzuki, K. Hyodo, H. Ishihara, H. Kikuchi, et al., Circadian clock in a mouse colon tumor regulates intracellular iron levels to promote tumor progression, J. Biol. Chem. 291 (13) (2016) 7017–7028.
[9] S. Khan, Y. Liu, R. Siddique, G. Nabi, M. Xue, H. Hou, Impact of chronically alternating light-dark cycles on circadian clock mediated expression of cancer (glioma)-related genes in the brain, Int. J. Biol. Sci. 15 (9) (2019) 1816–1834.
[10] W. Wei, W. Zhao, Y. Zhang, CBX4 provides an alternate mode of colon cancer development via potential influences on circadian rhythm and immune infiltration, Front. Cell Dev. Biol. 9 (2021) 669254.
[11] I. Aiello, M.L.M. Fedele, F. Roman, L. Marpegan, C. Caldart, J.J. Chiesa, D.A. Golombek, C.V. Finkielstein, N. Paladino, Circadian disruption promotes tumor-immune microenvironment remodeling favoring tumor cell proliferation, Sci. Adv. 6 (42) (2020).
[12] E. Hadadi, W. Taylor, X.M. Li, Y. Aslan, M. Villote, J. Riviere, G. Duvallet, C. Auriau, S. Dulong, I. Raymond-Letron, S. Provot, A. Bennaceur-Griscelli, H. Acloque, Chronic circadian disruption modulates breast cancer stemness and immune microenvironment to drive metastasis in mice, Nat. Commun. 11 (1) (2020) 3193.
[13] M. Yarchoan, A. Hopkins, E.M. Jaffee, Tumor mutational burden and response rate to PD-1 inhibition, N. Engl. J. Med. 377 (25) (2017) 2500–2501.
[14] P. Schmid, S. Adams, H.S. Rugo, A. Schneeweiss, C.H. Barrios, H. Iwata, V. Dieras, R. Hegg, S.A. Im, G. Shaw Wright, V. Henschel, L. Molinero, S.Y. Chui, et al., Atezolizumab and Nab-paclitaxel in advanced triple-negative breast cancer, N. Engl. J. Med. 379 (22) (2018) 2108–2121.
[15] M.E. Gatti-Mays, J.M. Balko, S.R. Gameiro, H.D. Bear, S. Prabhakaran, J. Fukui, M.L. Disis, R. Nanda, J.L. Gulley, K. Kalinsky, H. Abdul Sater, J.A. Sparano, D. Cescon, et al., If we build it they will come: targeting the immune response to breast cancer, NPJ Breast Cancer 5 (2019) 37.

[16] C. Liu, Y. Li, X. Xing, J. Zhuang, J. Wang, C. Wang, L. Zhang, L. Liu, F. Feng, H. Li, C. Gao, Y. Yu, J. Liu, et al., Immunogenomic landscape analyses of immune molecule signature-based risk panel for patients with triple-negative breast cancer, Mol. Ther. Nucleic Acids 28 (2022) 670–684.
[17] S. Burugu, K. Asleh-Aburaya, T.O. Nielsen, Immune infiltrates in the breast cancer microenvironment: detection, characterization and clinical implication, Breast Cancer 24 (1) (2017) 3–15.
[18] E. Farshadi, J. Yan, P. Leclere, A. Goldbeter, I. Chaves, G.T.J. van der Horst, The positive circadian regulators CLOCK and BMAL1 control G2/M cell cycle transition through Cyclin B1, Cell Cycle 18 (1) (2019) 16–33.
[19] P. Chen, R. Zhang, L. Mou, X. Li, Y. Qin, X. Li, An impaired hepatic clock system effects lipid metabolism in rats with nephropathy, Int. J. Mol. Med. 42 (5) (2018) 2720–2736.
[20] C. Dong, R. Gongora, M.L. Sosulski, F. Luo, C.G. Sanchez, Regulation of transforming growth factor-beta1 (TGF-beta1)-induced pro-fibrotic activities by circadian clock gene BMAL1, Respir. Res. 17 (2016) 4.
[21] L. Zhou, Y. Yu, S. Sun, T. Zhang, M. Wang, Cry 1 regulates the clock gene network and promotes proliferation and migration via the Akt/P53/P21 pathway in human osteosarcoma cells, J. Cancer 9 (14) (2018) 2480–2491.
[22] K.H. Cox, J.S. Takahashi, Circadian clock genes and the transcriptional architecture of the clock mechanism, J. Mol. Endocrinol. 63 (4) (2019) R93–R102.
[23] E. Reszka, S. Zienolddiny, Epigenetic basis of circadian rhythm disruption in cancer, Methods Mol. Biol. 1856 (2018) 173–201.
[24] J.S. Takahashi, Transcriptional architecture of the mammalian circadian clock, Nat. Rev. Genet. 18 (3) (2017) 164–179.
[25] C. Cadenas, L. van de Sandt, K. Edlund, M. Lohr, B. Hellwig, R. Marchan, M. Schmidt, J. Rahnenfuhrer, H. Oster, J.G. Hengstler, Loss of circadian clock gene expression is associated with tumor progression in breast cancer, Cell Cycle 13 (20) (2014) 3282–3291.
[26] Y. Ye, Y. Xiang, F.M. Ozguc, Y. Kim, C.J. Liu, P.K. Park, Q. Hu, L. Diao, Y. Lou, C. Lin, A.Y. Guo, B. Zhou, L. Wang, et al., The genomic landscape and pharmacogenomic interactions of clock genes in cancer chronotherapy, Cell Syst. 6 (3) (2018) 314–328 e312.
[27] C.H. Jung, E.M. Kim, J.K. Park, S.G. Hwang, S.K. Moon, W.J. Kim, H.D. Um, Bmal1 suppresses cancer cell invasion by blocking the phosphoinositide 3-kinase-Akt-MMP-2 signaling pathway, Oncol. Rep. 29 (6) (2013) 2109–2113.
[28] Z.L. Zeng, M.W. Wu, J. Sun, Y.L. Sun, Y.C. Cai, Y.J. Huang, L.J. Xian, Effects of the biological clock gene Bmal1 on tumour growth and anti-cancer drug activity, J. Biochem. 148 (3) (2010) 319–326.
[29] L. Xiao, A.K. Chang, M.X. Zang, H. Bi, S. Li, M. Wang, X. Xing, H. Wu, Induction of the CLOCK gene by E2-ERalpha signaling promotes the proliferation of breast cancer cells, PLoS One 9 (5) (2014) e95878.
[30] Y. Zhu, R.G. Stevens, D. Leaderer, A. Hoffman, T. Holford, Y. Zhang, H.N. Brown, T. Zheng, Non-synonymous polymorphisms in the circadian gene NPAS2 and breast cancer risk, Breast Cancer Res. Treat. 107 (3) (2008) 421–425.
[31] C.H. Yi, T. Zheng, D. Leaderer, A. Hoffman, Y. Zhu, Cancer-related transcriptional targets of the circadian gene NPAS2 identified by genome-wide ChIP-on-chip analysis, Cancer Lett. 284 (2) (2009) 149–156.
[32] Y. Wu, B. Tao, T. Zhang, Y. Fan, R. Mao, Pan-cancer analysis reveals disrupted circadian clock associates with T cell exhaustion, Front. Immunol. 10 (2019) 2451.
[33] M.H. Wang, X. Liu, Q. Wang, H.W. Zhang, A circadian rhythm-related gene signature for prognosis, invasion and immune microenvironment of breast cancer, Front. Genet. 13 (2022) 1104338.
[34] G. Stelzer, N. Rosen, I. Plaschkes, S. Zimmerman, M. Twik, S. Fishilevich, T.I. Stein, R. Nudel, I. Lieder, Y. Mazor, S. Kaplan, D. Dahary, D. Warshawsky, et al., The GeneCards suite: from gene data mining to disease genome sequence analyses, Curr. Protoc. Bioinf. 54 (2016) 1 30 31–31 30 33.
[35] K. Tomczak, P. Czerwinska, M. Wiznerowicz, The Cancer Genome Atlas (TCGA): an immeasurable source of knowledge, Contemp. Oncol. 19 (1A) (2015) A68–A77.
[36] J. Gao, B.A. Aksoy, U. Dogrusoz, G. Dresdner, B. Gross, S.O. Sumer, Y. Sun, A. Jacobsen, R. Sinha, E. Larsson, E. Cerami, C. Sander, N. Schultz, Integrative analysis of complex cancer genomics and clinical profiles using the cBioPortal, Sci. Signal. 6 (269) (2013) pl1.
[37] M.D. Wilkerson, D.N. Hayes, ConsensusClusterPlus: a class discovery tool with confidence assessments and item tracking, Bioinformatics 26 (12) (2010) 1572–1573.
[38] M.E. Ritchie, B. Phipson, D. Wu, Y. Hu, C.W. Law, W. Shi, G.K. Smyth, Limma powers differential expression analyses for RNA-sequencing and microarray studies, Nucleic Acids Res. 43 (7) (2015) e47.
[39] S. Hanzelmann, R. Castelo, J. Guinney, GSVA: gene set variation analysis for microarray and RNA-seq data, BMC Bioinf. 14 (2013) 7.
[40] G. Yu, L.G. Wang, Y. Han, Q.Y. He, clusterProfiler: an R package for comparing biological themes among gene clusters, OMICS 16 (5) (2012) 284–287.
[41] M. Ashburner, C.A. Ball, J.A. Blake, D. Botstein, H. Butler, J.M. Cherry, A.P. Davis, K. Dolinski, S.S. Dwight, J.T. Eppig, M.A. Harris, D.P. Hill, L. Issel-Tarver, et al., Gene ontology: tool for the unification of biology. The Gene Ontology Consortium, Nat. Genet. 25 (1) (2000) 25–29.
[42] H. Ogata, S. Goto, K. Sato, W. Fujibuchi, H. Bono, M. Kanehisa, KEGG: Kyoto Encyclopedia of genes and Genomes, Nucleic Acids Res. 27 (1) (1999) 29–34.
[43] K. Yoshihara, M. Shahmoradgoli, E. Martinez, R. Vegesna, H. Kim, W. Torres-Garcia, V. Trevino, H. Shen, P.W. Laird, D.A. Levine, S.L. Carter, G. Getz, K. Stemke-Hale, et al., Inferring tumour purity and stromal and immune cell admixture from expression data, Nat. Commun. 4 (2013) 2612.
[44] P. Jiang, S. Gu, D. Pan, J. Fu, A. Sahu, X. Hu, Z. Li, N. Traugh, X. Bu, B. Li, J. Liu, G.J. Freeman, M.A. Brown, et al., Signatures of T cell dysfunction and exclusion predict cancer immunotherapy response, Nat. Med. 24 (10) (2018) 1550–1558.
[45] P. Geeleher, N. Cox, R.S. Huang, pRRophetic: an R package for prediction of clinical chemotherapeutic response from tumor gene expression levels, PLoS One 9 (9) (2014) e107468.
[46] J. Friedman, T. Hastie, R. Tibshirani, Regularization paths for generalized linear models via coordinate descent, J. Stat. Software 33 (1) (2010) 1–22.
[47] M. Uhlen, C. Zhang, S. Lee, E. Sjostedt, L. Fagerberg, G. Bidkhori, R. Benfeitas, M. Arif, Z. Liu, F. Edfors, K. Sanli, K. von Feilitzen, P. Oksvold, et al., A pathology atlas of the human cancer transcriptome, Science 357 (6352) (2017).
[48] W. Shen, Z. Song, X. Zhong, M. Huang, D. Shen, P. Gao, X. Qian, M. Wang, X. He, T. Wang, S. Li, X. Song, Sangerbox: a comprehensive, interaction-friendly clinical bioinformatics analysis platform, iMeta 1 (3) (2022) e36.
[49] A.J. Vickers, A.M. Cronin, E.B. Elkin, M. Gonen, Extensions to decision curve analysis, a novel method for evaluating diagnostic tests, prediction models and molecular markers, BMC Med. Inf. Decis. Making 8 (2008) 53.
[50] A. Mayakonda, D.C. Lin, Y. Assenov, C. Plass, H.P. Koeffler, Maftools: efficient and comprehensive analysis of somatic variants in cancer, Genome Res. 28 (11) (2018) 1747–1756.
[51] C.J. Liu, F.F. Hu, M.X. Xia, L. Han, Q. Zhang, A.Y. Guo, GSCALite: a web server for gene set cancer analysis, Bioinformatics 34 (21) (2018) 3771–3772.
[52] J.D. Storey, R. Tibshirani, Statistical significance for genomewide studies, Proc. Natl. Acad. Sci. U. S. A. 100 (16) (2003) 9440–9445.
[53] B. Park, J. Im, K. Han, Comparative analysis of gene correlation networks of breast cancer patients based on mutations in TP53, Biomolecules 12 (7) (2022).
[54] Y.H. He, M.H. Yeh, H.F. Chen, T.S. Wang, R.H. Wong, Y.L. Wei, T.K. Huynh, D.W. Hu, F.J. Cheng, J.Y. Chen, S.W. Hu, C.C. Huang, Y. Chen, et al., ERalpha determines the chemo-resistant function of mutant p53 involving the switch between lincRNA-p21 and DDB2 expressions, Mol. Ther. Nucleic Acids 25 (2021) 536–553.
[55] A.B. Hanker, B.P. Brown, J. Meiler, A. Marin, H.S. Jayanthan, D. Ye, C.C. Lin, H. Akamatsu, K.M. Lee, S. Chatterjee, D.R. Sudhan, A. Servetto, M.R. Brewer, et al., Co-occurring gain-of-function mutations in HER2 and HER3 modulate HER2/HER3 activation, oncogenesis, and HER2 inhibitor sensitivity, Cancer Cell 39 (8) (2021) 1099–1114 e1098.
[56] K. Lee, J. Lee, J. Choi, S.H. Sim, J.E. Kim, M.H. Kim, Y.H. Park, J.H. Kim, S.J. Koh, K.H. Park, M.J. Kang, M.S. Ahn, K.E. Lee, et al., Genomic analysis of plasma circulating tumor DNA in patients with heavily pretreated HER2 + metastatic breast cancer, Sci. Rep. 13 (1) (2023) 9928.
[57] S. Abelson, A.G.X. Zeng, I. Nofech-Mozes, T.T. Wang, S.W.K. Ng, M.D. Minden, T.J. Pugh, P. Awadalla, L.I. Shlush, T. Murphy, S.M. Chan, J.E. Dick, S. V. Bratman, Integration of intra-sample contextual error modeling for improved detection of somatic mutations from deep sequencing, Sci. Adv. 6 (50) (2020).
[58] Z. Li, H. Zhang, X. Wang, Q. Wang, J. Xue, Y. Shi, M. Wang, G. Wang, J. Zhang, Identification of cuproptosis-related subtypes, characterization of tumor microenvironment infiltration, and development of a prognosis model in breast cancer, Front. Immunol. 13 (2022) 996836.

[59] D. Khandekar, D.O. Dahunsi, I.V. Manzanera Esteve, S. Reid, J.C. Rathmell, J. Titze, V. Tiriveedhi, Low-salt diet reduces anti-CTLA4 mediated systemic immune-related adverse events while retaining therapeutic efficacy against breast cancer, Biology 11 (6) (2022).
[60] X. Ke, H. Wu, Y.X. Chen, Y. Guo, S. Yao, M.R. Guo, Y.Y. Duan, N.N. Wang, W. Shi, C. Wang, S.S. Dong, H. Kang, Z. Dai, et al., Individualized pathway activity algorithm identifies oncogenic pathways in pan-cancer analysis, EBioMedicine 79 (2022) 104014.
[61] Y. Xie, Q. Tang, G. Chen, M. Xie, S. Yu, J. Zhao, L. Chen, New insights into the circadian rhythm and its related diseases, Front. Physiol. 10 (2019) 682.
[62] R.V. Puram, M.S. Kowalczyk, C.G. de Boer, R.K. Schneider, P.G. Miller, M. McConkey, Z. Tothova, H. Tejero, D. Heckl, M. Jaras, M.C. Chen, H. Li, A. Tamayo, et al., Core circadian clock genes regulate leukemia stem cells in AML, Cell 165 (2) (2016) 303–316.
[63] D.E. Blask, S.M. Hill, R.T. Dauchy, S. Xiang, L. Yuan, T. Duplessis, L. Mao, E. Dauchy, L.A. Sauer, Circadian regulation of molecular, dietary, and metabolic signaling mechanisms of human breast cancer growth by the nocturnal melatonin signal and the consequences of its disruption by light at night, J. Pineal Res. 51 (3) (2011) 259–269.
[64] Y. Liu, S. Guo, Y. Sun, C. Zhang, J. Gan, S. Ning, J. Wang, CRS: a circadian rhythm score model for predicting prognosis and treatment response in cancer patients, J. Transl. Med. 21 (1) (2023) 185.
[65] E. Borcoman, P. De La Rochere, W. Richer, S. Vacher, W. Chemlali, C. Krucker, N. Sirab, F. Radvanyi, Y. Allory, G. Pignot, N. Barry de Longchamps, D. Damotte, D. Meseure, et al., Inhibition of PI3K pathway increases immune infiltrate in muscle-invasive bladder cancer, OncoImmunology 8 (5) (2019) e1581556.
[66] Y.T. Liu, Z.J. Sun, Turning cold tumors into hot tumors by improving T-cell infiltration, Theranostics 11 (11) (2021) 5365–5386.
[67] J. Li, K.T. Byrne, F. Yan, T. Yamazoe, Z. Chen, T. Baslan, L.P. Richman, J.H. Lin, Y.H. Sun, A.J. Rech, D. Balli, C.A. Hay, Y. Sela, et al., Tumor cell-intrinsic factors underlie heterogeneity of immune cell infiltration and response to immunotherapy, Immunity 49 (1) (2018) 178–193 e177.
[68] M. Desbois, Y. Wang, Cancer-associated fibroblasts: key players in shaping the tumor immune microenvironment, Immunol. Rev. 302 (1) (2021) 241–258.
[69] Y. Wu, Z. Yi, J. Li, Y. Wei, R. Feng, J. Liu, J. Huang, Y. Chen, X. Wang, J. Sun, X. Yin, Y. Li, J. Wan, et al., FGFR blockade boosts T cell infiltration into triple-negative breast cancer by regulating cancer-associated fibroblasts, Theranostics 12 (10) (2022) 4564–4580.
[70] R.L. Barrett, E. Pure, Cancer-associated fibroblasts and their influence on tumor immunity and immunotherapy, Elife 9 (2020).
[71] E. Sahai, I. Astsaturov, E. Cukierman, D.G. DeNardo, M. Egeblad, R.M. Evans, D. Fearon, F.R. Greten, S.R. Hingorani, T. Hunter, R.O. Hynes, R.K. Jain, T. Janowitz, et al., A framework for advancing our understanding of cancer-associated fibroblasts, Nat. Rev. Cancer 20 (3) (2020) 174–186.
[72] J.P. DeBruyne, J.E. Baggs, T.K. Sato, J.B. Hogenesch, Ubiquitin ligase Siah2 regulates RevErbalpha degradation and the mammalian circadian clock, Proc. Natl. Acad. Sci. U. S. A. 112 (40) (2015) 12420–12425.
[73] M.G. Adam, S. Matt, S. Christian, H. Hess-Stumpp, A. Haegebarth, T.G. Hofmann, C. Algire, SIAH ubiquitin ligases regulate breast cancer cell migration and invasion independent of the oxygen status, Cell Cycle 14 (23) (2015) 3734–3747.
[74] Q. Liu, Q. Luo, J. Feng, Y. Zhao, B. Ma, H. Cheng, T. Zhao, H. Lei, C. Mu, L. Chen, Y. Meng, J. Zhang, Y. Long, et al., Hypoxia-induced proteasomal degradation of DBC1 by SIAH2 in breast cancer progression, Elife 11 (2022).
[75] J. Xu, W. Zhang, EZR promotes pancreatic cancer proliferation and metastasis by activating FAK/AKT signaling pathway, Cancer Cell Int. 21 (1) (2021) 521.
[76] Y. Xiao, G. Liu, Y. Sun, Y. Gao, X. Ouyang, C. Chang, L. Gong, S. Yeh, Targeting the estrogen receptor alpha (ERalpha)-mediated circ-SMG1.72/miR-141-3p/Gelsolin signaling to better suppress the HCC cell invasion, Oncogene 39 (12) (2020) 2493–2508.
[77] X. Sun, Z. Wang, X. Chen, K. Shen, CRISPR-cas9 screening identified lethal genes enriched in cell cycle pathway and of prognosis significance in breast cancer, Front. Cell Dev. Biol. 9 (2021) 646774.
[78] A.C. Rutkovsky, E.S. Yeh, S.T. Guest, V.J. Findlay, R.C. Muise-Helmericks, K. Armeson, S.P. Ethier, Eukaryotic initiation factor 4E-binding protein as an oncogene in breast cancer, BMC Cancer 19 (1) (2019) 491.
[79] G. Davies, G.H. Cunnick, R.E. Mansel, M.D. Mason, W.G. Jiang, Levels of expression of endothelial markers specific to tumour-associated endothelial cells and their correlation with prognosis in patients with breast cancer, Clin. Exp. Metastasis 21 (1) (2004) 31–37.
[80] H. Yang, F. Zhang, H. Long, Y. Lin, J. Liao, H. Xia, K. Huang, IFT20 mediates the transport of cell migration regulators from the trans-golgi network to the plasma membrane in breast cancer cells, Front. Cell Dev. Biol. 9 (2021) 632198.
[81] X. Zheng, S. Chen, Q. Yang, J. Cai, W. Zhang, H. You, J. Xing, Y. Dong, Salvianolic acid A reverses the paclitaxel resistance and inhibits the migration and invasion abilities of human breast cancer cells by inactivating transgelin 2, Cancer Biol. Ther. 16 (9) (2015) 1407–1414.
[82] M. Bajor, A.O. Zych, A. Graczyk-Jarzynka, A. Muchowicz, M. Firczuk, L. Trzeciak, P. Gaj, A. Domagala, M. Siernicka, A. Zagozdzon, P. Siedlecki, M. Kniotek, P. C. O'Leary, et al., Targeting peroxiredoxin 1 impairs growth of breast cancer cells and potently sensitises these cells to prooxidant agents, Br. J. Cancer 119 (7) (2018) 873–884.
[83] M.B. Hampton, K.A. Vick, J.J. Skoko, C.A. Neumann, Peroxiredoxin involvement in the initiation and progression of human cancer, Antioxidants Redox Signal. 28 (7) (2018) 591–608.
[84] P.C. O'Leary, M. Terrile, M. Bajor, P. Gaj, B.T. Hennessy, G.B. Mills, A. Zagozdzon, D.P. O'Connor, D.J. Brennan, K. Connor, J. Li, A.M. Gonzalez-Angulo, H. D. Sun, et al., Peroxiredoxin-1 protects estrogen receptor alpha from oxidative stress-induced suppression and is a protein biomarker of favorable prognosis in breast cancer, Breast Cancer Res. 16 (4) (2014) R79.
[85] T.A. Chan, M. Yarchoan, E. Jaffee, C. Swanton, S.A. Quezada, A. Stenzinger, S. Peters, Development of tumor mutation burden as an immunotherapy biomarker: utility for the oncology clinic, Ann. Oncol. 30 (1) (2019) 44–56.
[86] J. Wang, X. Zhang, J. Li, X. Ma, F. Feng, L. Liu, J. Wu, C. Sun, ADRB1 was identified as a potential biomarker for breast cancer by the co-analysis of tumor mutational burden and immune infiltration, Aging 13 (1) (2020) 351–363.